

Strongly correlated systems  
in atomic and condensed matter physics

Lecture notes for Physics 284

by Eugene Demler

Harvard University

September 22, 2014



## Chapter 7

# Bose Hubbard model

### 7.1 Qualitative arguments

We consider spinless bosonic atoms in an optical lattice with repulsive interaction between atoms[11]. They can be described by the Bose Hubbard model[9].

$$\mathcal{H} = -t \sum_{\langle ij \rangle} b_i^\dagger b_j + \frac{U}{2} \sum_i n_i (n_i - 1) - \mu \sum_i n_i \quad (7.1)$$

We have on-site interaction only since particles have contact interaction and we assume tight-binding limit. Away from the tight-binding regime, and especially for shallower lattices, one may need to include non-local interactions. In the presence of confining potential we also need to include

$$\mathcal{H}_{\text{pot}} = \sum_i V(r_i) n_i \quad (7.2)$$

Parameters  $t$  and  $U$  can be controlled by selecting the strength of the optical lattice and tuning the scattering length with magnetic field.

We discuss two limiting cases first.

*Weak interactions regime*  $t \gg U$ .

Atoms condense into the state of the lowest kinetic energy

$$|\Psi_{\text{SF}}\rangle = \frac{1}{\sqrt{N!}} (b_{k=0}^\dagger)^{N_{\text{at}}} |0\rangle \approx c e^{\sqrt{N_{\text{at}}} b_{k=0}^\dagger} |0\rangle \quad (7.3)$$

Here  $|0\rangle$  is the vacuum state with no particles. State (6.3) is a superfluid state. We can also write

$$b_{k=0}^\dagger = \frac{1}{\sqrt{N_{\text{sites}}}} \sum_i b_i^\dagger \quad (7.4)$$

to write

$$|\Psi_{\text{SF}}\rangle = c \prod_i e^{\sqrt{\frac{N_{\text{atoms}}}{N_{\text{sites}}}} b_i^\dagger} \quad (7.5)$$

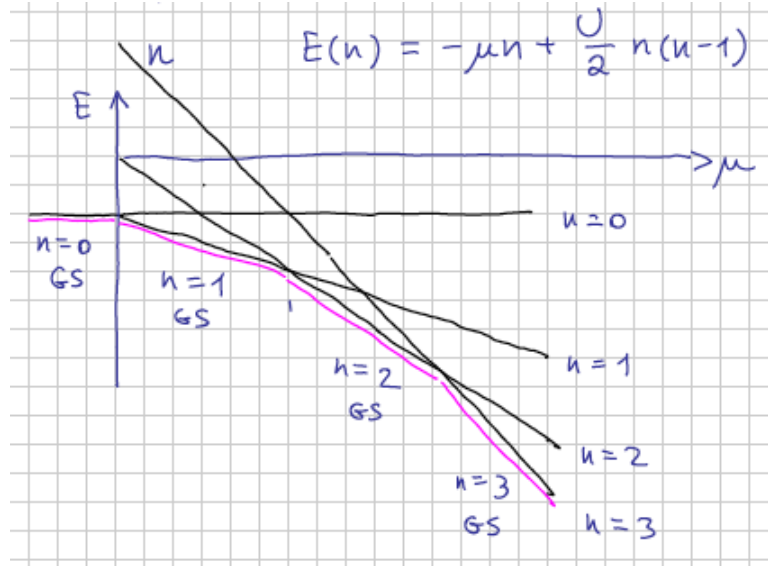


Figure 7.1: Bose Hubbard model with  $t = 0$ . Level crossings between states with different atom numbers.

*Strong interactions regime  $t \ll U$ .*

Interaction term in the Hamiltonian plays the dominant role. As a first step let us take  $t = 0$ .

$$\mathcal{H}_U + \mathcal{H}_\mu = \frac{U}{2} \sum_i n_i (n_i - 1) - \mu \sum_i n_i \quad (7.6)$$

Different sites are now decoupled. Eigenstates in each well have a well defined number of particles. For an individual well we can write

$$\begin{array}{ll} n &= 0 & E &= 0 \\ n &= 1 & E &= -\mu \\ n &= 2 & E &= -2\mu + U \\ n &= 3 & E &= -3\mu + 3U \\ n &= 4 & E &= -4\mu + 4U \\ &\dots & & \\ n & & E_n &= -n\mu + \frac{U}{2}n(n-1) \end{array} \quad (7.7)$$

The ground state has  $n$  bosons when

$$(n-1)U < \mu < nU \quad (7.8)$$

There are level crossing between states with different integer fillings for  $\mu = nU$ . Away from level crossings these states have a gap. Hence they should be stable against small changes in the Hamiltonian, such as small tunneling. These are insulating Mott states.

## 7.2 Gutzwiller variational wavefunctions

To describe transitions between the superfluid and insulating states we use Gutzwiller variational wavefunction

$$|\Psi_G\rangle = \prod_i \left( f_0 + f_1 b_i^\dagger + f_2 \frac{b_i^{\dagger 2}}{\sqrt{2}} + \cdots + f_n \frac{b_i^{\dagger n}}{\sqrt{n!}} \right) |0\rangle \quad (7.9)$$

This wavefunction requires normalization condition

$$\sum_n |f_n|^2 = 1 \quad (7.10)$$

Our justification for using the Gutzwiller ansatz is that a factorizable wavefunction works in both extreme limits: deep in the superfluid state and deep in the Mott state. It is natural to assume that this wavefunction will work near the transition point as well. It turns out that this wavefunction is quite accurate in  $d=3$ , but in lower dimensions it works only qualitatively. The transition point obtained from the MC analysis is sufficiently different from the one predicted by the Gutzwiller ansatz. This is not surprising since this is essentially the mean-field analysis which becomes increasingly better in higher dimensions.

We need to minimize the wavefunction (6.9) with respect to  $f_n$  subject to the constraint (6.10).

Interaction energy

$$\langle \mathcal{H}_U + \mathcal{H}_\mu \rangle = -\mu |f_1|^2 + (2\mu + U) |f_2|^2 + \cdots + (-n\mu + \frac{U}{2} n(n-1)) |f_n|^2 + \cdots \quad (7.11)$$

Kinetic energy

$$\mathcal{H}_t = -zt |f_0^* f_1 + \sqrt{2} f_1^* f_2 + \sqrt{3} f_2^* f_3 + \cdots|^2 \quad (7.12)$$

Interaction energy favors a fixed number of particles per well, while the kinetic energy favors a coherent superposition of the number states. To understand the transition let us consider the stability of the Mott state with  $n$  particles (at a fixed density). We take the Gutzwiller wavefunction with

$$f_n = (1 - 2\alpha^2)^{1/2} \quad f_{n-1} = f_{n+1} = \alpha \quad (7.13)$$

here  $\alpha$  is assumed to be small and all other  $f_i$  are zero. We expand the energy up to the second order in  $\alpha$

$$\mathcal{H}_t = -zt |\alpha (1 - 2\alpha^2)^{1/2} \sqrt{n} + \alpha (1 - 2\alpha^2)^{1/2} \sqrt{n+1}|^2 \approx -zt \alpha^2 |\sqrt{n} + \sqrt{n+1}|^2 \quad (7.14)$$

We take the middle of the Mott plateau

$$\mu = U(n - 1/2) \quad (7.15)$$

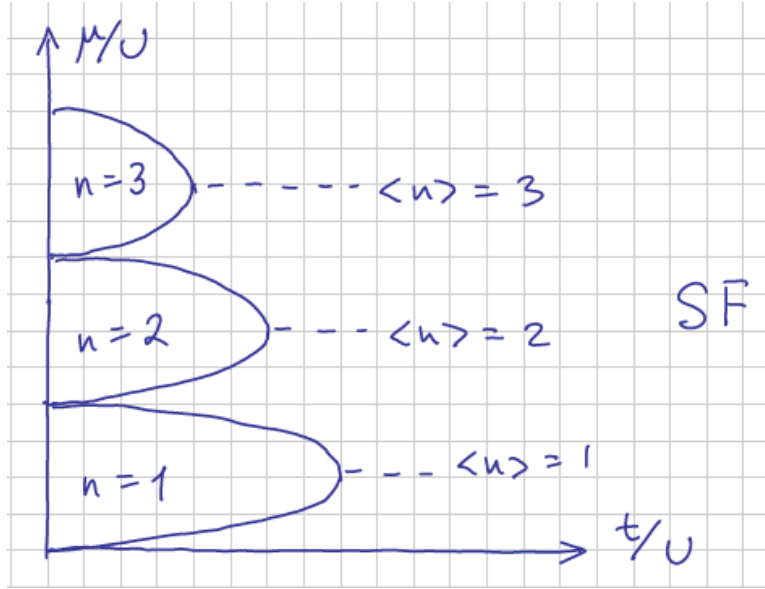


Figure 7.2: Phase diagram of the Bose Hubbard model according to the Gutzwiller variational wavefunction.

We have for the relevant number states

$$\begin{aligned}\langle \mathcal{H}_U + \mathcal{H}_\mu \rangle_n &= \frac{U}{2}n(n-1) - U(n-1/2)n = -\frac{U}{2}n^2 \\ \langle \mathcal{H}_U + \mathcal{H}_\mu \rangle_{n-1} &= \frac{U}{2}(n-1)(n-2) - U(n-1/2)(n-1) = -\frac{U}{2}(n^2-1) \\ \langle \mathcal{H}_U + \mathcal{H}_\mu \rangle_{n+1} &= \frac{U}{2}(n-1)n - U(n-1/2)(n+1) = -\frac{U}{2}(n^2-1)\end{aligned}\quad (7.16)$$

Thus we find

$$E_{\text{tot}}(\alpha) = -zt\alpha^2 |\sqrt{n} + \sqrt{n+1}|^2 + \frac{U}{2}2\alpha^2 + \dots \quad (7.17)$$

The Mott to Superfluid transition takes place when the coefficient in front of  $\alpha^2$  becomes negative. For large  $n$  this corresponds to

$$U = 4nzt \quad (7.18)$$

Note that the Mott state exists only for integer filling factors. For  $\langle n \rangle = N + \epsilon$ , even when  $N$  atoms become localized,  $\epsilon$  makes a superfluid state even for the smallest values of tunneling.

Confining parabolic potential acts as a cut through the phase diagram. Hence in a parabolic potential we find a "wedding cake" structure of shells.

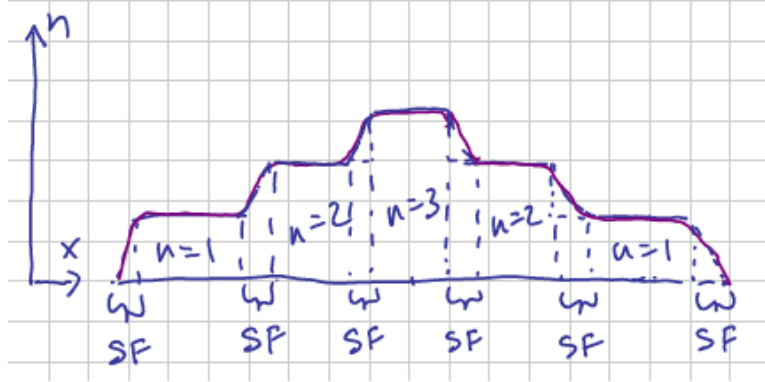


Figure 7.3: Density distribution of atoms in an optical lattice in the Hubbard regime. Incompressible Mott states give rise to the flat plateaus. Compressible superfluid shells make regions where the density is changing smoothly.

### 7.3 Experiments on the superfluid to Mott transition in optical lattices

Superfluid to Mott insulator transition for ultracold atoms in optical lattices was first demonstrated by Greiner et al. [1] (see fig. 6.4). They use TOF experiments to measure occupation numbers in momentum space  $n_k = b_k^\dagger b_k$ , where  $k$  is the physical momentum. In the SF state we have macroscopic occupation of the state with the lowest kinetic energy. In a lattice a state with the lowest kinetic energy is a state with quasi-momentum zero. Quasi-momentum differs from the physical momentum by Bragg reflections. So in the SF state atoms should exhibit macroscopic occupation of states with momenta equal to reciprocal lattice vectors. One can also understand this result as constructive interference from a periodic array of coherent sources. Finite size of wavefunctions in individual wells determines how many Bragg peaks can be observed. In the Mott state one occupies all quasimomenta so expansion images do not have sharp peaks. We can also say that we no longer have coherent sources so interference is lost. There has been a certain controversy regarding finite width of the peaks. It was suggested that this was due to the high temperature in the system, thus experiments could not be considered a demonstration of the quantum phase transition. Detailed analysis showed that this can be explained by the finite TOF expansion time [2].

Considerable effort was also dedicated to observing the "wedding cake" structure in a parabolic potential. Recent experiments reached single site resolution and provided convincing demonstration of the incompressible Mott plateaus and the wedding cake structure [4, 8, 3] (see fig. 6.5). Note that these experiments can be used to measure not only the average number of particles, but also fluctuations. In the superfluid state we expect to see much large fluctuations since they correspond to a superposition of several number states.

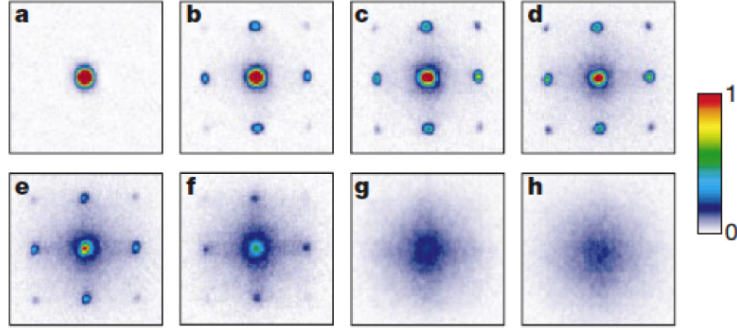


Figure 7.4: Demonstration of the superfluid to insulator transition with bosons in an optical lattice[1]. These TOF experiments measure occupation number in momentum space  $n_k = b_k^\dagger b_k$ . In the superfluid state there is macroscopic occupation of the state with the lattice quasimomentum equal to zero. In TOF this shows up as peaks for momenta that correspond to reciprocal lattice vectors. In the Mott state all quasimomenta are occupied.

## 7.4 Collective modes in Bose Hubbard model

### 7.4.1 Superfluid state

In the superfluid phase we have an order parameter  $\langle b_i \rangle = |\Phi|e^{i\phi}$ . We expect two types of collective mode: phase fluctuations correspond to gapless Bogoliubov-like excitations. This is the Goldstone mode of the spontaneously broken symmetry. Fluctuations of the amplitude of the order parameter correspond to a massive Higgs like mode (see fig. 6.6). We discuss simple analysis that illustrates the appearance of these modes.

We consider a variational wavefunction in which we keep states with  $n - 1$ ,  $n$ , and  $n + 1$  particles only.

$$|\Psi\rangle = \prod_i [e^{-i\chi_i} \cos \theta_i (e^{-i\phi_i} \sin(\gamma_i) |n-1\rangle + e^{i\phi_i} \cos(\gamma_i) |n+1\rangle) + e^{i\chi_i} \sin \theta_i |n\rangle]_i \quad (7.19)$$

We are interested in states with the average number of atoms per site  $n$ , hence  $\gamma$  should be close to  $\pi/4$ . We introduce  $\gamma = \frac{\pi}{4} - \sigma$ . Truncating the Gutzwiller wavefunction to only three Fock (number) states is a reasonable approximation close to the superfluid to Mott transition, where number fluctuations are small. For simplicity, we will also assume that  $n$  is large so we can neglect the difference between  $n$  and  $n \pm 1$ .

First we do the mean-field analysis for the wavefunction (6.19). The minimum energy state requires  $\chi = 0$ ,  $\phi$  arbitrary but uniform, and  $\sigma = 0$  when the density



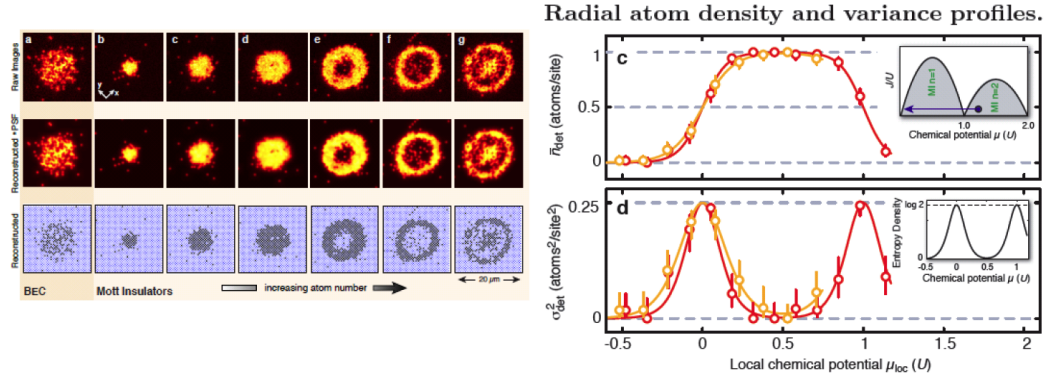


Figure 7.5: Wedding cake structure in a parabolic potential[3]. In these experiments the number of particles in individual wells is measured modulo two. In other words two particles appear as zero, three particles appear as one. Figures show both the average number of particles and the variance. The variance is large in the superfluid shells.

is precisely  $n$ . Energy as a function of  $\theta$

$$E = -\frac{nz t}{2} \sin^2 \theta + \frac{U}{2} \cos^2 \theta \quad (7.20)$$

Minimizing with respect to  $\theta$  we find that when  $U > 4nzt$  we have a Mott state with  $\theta = \pi/2$ , when  $U < 4nzt$  we find a superfluid state with

$$\cos 2\theta_0 = -U/4nzt \quad (7.21)$$

Our goal is to project dynamics into the variational state (6.19) and analyze collective modes. Let us consider the Lagrangian defined as

$$L = \langle \Psi(t) | (-i) \partial_t + \mathcal{H} | \Psi(t) \rangle \quad (7.22)$$

If  $|\Psi(t)\rangle$  was arbitrary, by finding an extremum of  $L$  with respect to  $|\Psi(t)\rangle$  we would recover the Schroedinger equation. To find projected dynamics we assume that wavefunctions in (6.22) are limited to the class of wavefunctions described by equation (6.19) and look for the extremum of  $L$  [10, 6]. All parameters in (6.19) are functions of time and can be different at different sites. To find the extremum of  $L$  one can write equations of motion for individual variables  $d_t \partial_{q_i} L = \partial_{q_i} L$ , where  $q_i$  stands for all variables in (6.19). Since we are interested in collective modes only, we consider small fluctuations around the equilibrium state (6.21) and expand up to quadratic order in  $\sigma_i$ ,  $\chi_i$ ,  $\delta\theta_i = \theta_i - \theta_0$ . Moreover we are interested in the long wavelength behavior of collective modes. Thus our plan is to get the continuum limit of  $L$  first and then write equations of motion.

We have

$$\langle \Psi(t) | (-i) \partial_t | \Psi(t) \rangle = \sum_i [\cos 2\theta_0 \dot{\chi}_i - 2 \sin 2\theta_0 \delta\theta \dot{\chi}_i + 2 \sin^2 \theta_0 \sigma \dot{\phi}_i] \quad (7.23)$$

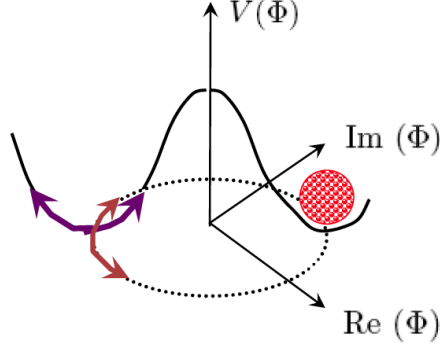


Figure 7.6: Schematic illustration of the origin of two modes in the superfluid state. A state of broken symmetry can be represented as residing in the trough of the "Mexican hat" potential. Fluctuations of the phase of the order parameter correspond to moving along the bottom of the trough. They give rise to the gapless Bogoliubov mode. Fluctuations in the magnitude of the order parameter ("uphill" with respect to the potential) correspond to the gapped amplitude (Higgs) excitation.

The part of (6.22) with the Hamiltonian is more subtle so let us discuss it in more details

$$\begin{aligned}
 \langle \Psi(t) | \mathcal{H}_{\text{kin}} | \Psi(t) \rangle &= -nt \sum_{\langle ij \rangle} \sin \theta_i \cos \theta_i \sin \theta_j \cos \theta_j \\
 &\times \left\{ [\cos \gamma_i e^{i(\phi_i - \chi_i)} + \sin \gamma_i e^{i(\phi_i + \chi_i)}] [\cos \gamma_j e^{-i(\phi_j - \chi_j)} + \sin \gamma_j e^{-i(\phi_j + \chi_j)}] + \text{c.c.} \right\}
 \end{aligned} \tag{7.24}$$

We have

$$\begin{aligned}
 \sin \theta_i \cos \theta_i \sin \theta_j \cos \theta_j &= \frac{1}{4} \sin(2\theta_0 + 2\delta\theta_i) \sin(2\theta_0 + 2\delta\theta_j) \\
 &\approx \frac{1}{4} \sin^2 2\theta_0 + \frac{1}{4} \sin 4\theta_0 (\delta\theta_i + \delta\theta_j) + \frac{1}{2} \cos 4\theta_0 (\delta\theta_i^2 + \delta\theta_j^2) - \frac{1}{2} \cos^2 2\theta_0 (\delta\theta_i - \delta\theta_j)^2
 \end{aligned} \tag{7.25}$$

and

$$\begin{aligned}
 &[ \cos(\frac{\pi}{4} + \sigma_i) e^{i(\phi_i - \chi_i)} + \sin(\frac{\pi}{4} + \sigma_i) e^{i(\phi_i + \chi_i)} ] [ \cos(\frac{\pi}{4} + \sigma_j) e^{-i(\phi_j - \chi_j)} + \sin(\frac{\pi}{4} + \sigma_j) e^{-i(\phi_j + \chi_j)} ] + \text{c.c.} \\
 &\approx \frac{1}{2} (2 - \sigma_i^2 - \phi_i^2 - \chi_i^2 + 2i\phi_i + 2i\sigma_i\chi_i) (2 - \sigma_j^2 - \phi_j^2 - \chi_j^2 - 2i\phi_j + 2i\sigma_j\chi_j) + \text{c.c.} \\
 &= 4 - 2[\chi_i^2 + \chi_j^2 + \sigma_i^2 + \sigma_j^2 + (\phi_i - \phi_j)^2]
 \end{aligned} \tag{7.26}$$

Hence

$$\begin{aligned}
& \langle \Psi(t) | \mathcal{H}_{\text{kin}} | \Psi(t) \rangle = -N_{\text{sites}} n z t \sin^2 2\theta_0 \\
& - n t \sin 4\theta_0 \sum_{\langle ij \rangle} (\delta\theta_i + \delta\theta_j) - 2nt \cos 4\theta_0 \sum_{\langle ij \rangle} (\delta\theta_i^2 + \delta\theta_j^2) + 2nt \cos^2 2\theta_0 \sum_{\langle ij \rangle} (\delta\theta_i - \delta\theta_j)^2 \\
& + \frac{nt}{2} \sin^2 2\theta_0 \sum_{\langle ij \rangle} [\chi_i^2 + \chi_j^2 + \sigma_i^2 + \sigma_j^2 + (\phi_i - \phi_j)^2]
\end{aligned} \tag{7.27}$$

Here  $z$  is the coordination number. And we also find

$$\begin{aligned}
& \langle \Psi(t) | \mathcal{H}_U + \mathcal{H}_\mu | \Psi(t) \rangle = \frac{U}{2} \sum_i \cos^2 \theta_i = \frac{U}{4} \sum_i \cos(2\theta_0 + 2\delta\theta_i) + \text{const} \\
& = \frac{N_{\text{sites}} U}{4} \cos 2\theta_0 - \frac{U}{2} \sin 2\theta_0 \sum_i \delta\theta_i - \frac{U}{2} \cos 2\theta_0 \sum_i \delta\theta_i^2
\end{aligned} \tag{7.28}$$

To analyze long wavelength excitations we take the continuum limit of this expression. This means

$$\begin{aligned}
\sum_{ij} (\sigma_i^2 + \sigma_j^2) &= \frac{z}{a^d} \int dx^d \sigma^2(x) \\
\sum_{ij} (\phi_i - \phi_j)^2 &= \frac{1}{a^{d-2}} \int dx^d (\nabla \phi(x))^2
\end{aligned} \tag{7.29}$$

Here  $a$  is a lattice constant which we will set equal to one.

Thus we find for the relevant part of the lagrangian

$$\begin{aligned}
L &= \int d^d x \left( -2 \sin 2\theta_0 \delta\theta \dot{\chi} + 2 \sin^2 \theta_0 \sigma \dot{\phi} \right) \\
&- \left( 2nzt \cos 4\theta_0 + \frac{U}{2} \cos 2\theta_0 \right) \int d^d x (\delta\theta)^2 + 2nt \cos^2 2\theta_0 \int d^d x (\nabla \delta\theta)^2 \\
&+ \frac{znt \sin^2 2\theta_0}{2} \int d^d x [\chi^2 + \sigma^2] + \frac{nt \sin^2 2\theta_0}{2} \int d^d x (\nabla \phi)^2
\end{aligned} \tag{7.30}$$

Note that terms linear in fluctuating fields canceled because we expanded around a state that satisfies the mean-field minimization procedure. We also omitted the first term in (6.23) since it corresponds to the integral of the time derivative and does not change equations of motion.

Equations of motion separate into two coupled pairs. The first pair corresponds to the usual superfluid hydrodynamics: continuity equation and Josephson relation between the rate of phase winding and the change in the chemical potential

$$\begin{aligned}
2 \sin^2 \theta_0 \dot{\sigma} &= -nt \sin^2 2\theta_0 \nabla^2 \phi \\
2 \sin^2 \theta_0 \dot{\phi} &= -znt \sin^2 2\theta_0 \sigma
\end{aligned} \tag{7.31}$$

The second pair of equations is less familiar

$$\begin{aligned} -2 \sin 2\theta_0 \delta \dot{\theta} &= znt \sin^2 2\theta_0 \chi \\ -2 \sin 2\theta_0 \dot{\chi} - 2(2nzt \cos 4\theta_0 + \frac{U}{2} \cos 2\theta_0) \delta \theta - 4nt \cos^2 2\theta_0 \nabla^2 \delta \theta &= 0 \end{aligned} \quad (7.32)$$

From equations (6.31) we find

$$\ddot{\phi} = 4z(nt)^2 \cos^4 \theta_0 \nabla^2 \phi \quad (7.33)$$

This equation describes the phase mode (= Bogoliubov mode = Goldstone mode) with  $\omega_k = v|k|$ . From equations (6.32) we obtain

$$\ddot{\theta} = -\omega_0^2 \theta + \alpha \nabla^2 \theta \quad (7.34)$$

with

$$\omega_0^2 = \frac{(4nzt)^2 - U^2}{32} \quad (7.35)$$

This corresponds to a massive amplitude (Higgs) mode  $\omega_k = \omega_0 + \alpha k^2$ . Note that at the transition point into the Mott phase  $U = 4znt$  and the energy of the amplitude mode goes to zero. Such mode softening is expected generically at a continuous quantum phase transition.

Analysis presented above can be easily extended away from the long-wavelength limit. The full spectrum of collective modes is shown in figure 6.8.

### 7.4.2 Mott state

In the insulating state we find particle- and hole-like collective modes (see fig. 6.7). If we take middle of the Mott plateau with  $\mu_0 = U(n - \frac{1}{2})$  we find that energies of these excitations are  $E_k = \frac{U}{2} - 2nt(\cos k_x + \cos k_y + \cos k_z)$ . This is the particle-hole symmetric case. At the transition point into the SF state the energy of both p- and h-like excitations goes to zero. So the SF state can be thought of as a result of Bose condensation of p- and h-like excitations

Away from the p-h symmetric case, when  $\mu = \mu_0 + \delta\mu$  energies of particle- and hole-like excitations differ  $E_{\{p,h\}k} = \frac{U}{2} - 2nt(\cos k_x + \cos k_y + \cos k_z) \mp \delta\mu$ .

The spectrum of excitations in the Mott state is shown in figure 6.8.

### 7.4.3 Probing collective modes

The first experiments probing collective modes in an optical lattice were lattice modulation experiments performed by Stoferle et al [13] (see fig. 6.10). In the Mott state the system can only be excited by creating particle-hole excitations, which requires energy  $U$ . Thus we see peaks at finite energy. In the superfluid state we have gapless excitations so one would naively expect that we should see response at low frequencies. But this is not what we see in experiments. There are two important factors. Firstly, lattice modulation is a translationally

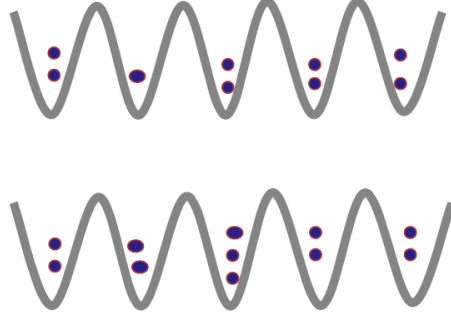


Figure 7.7: Schematic representation of excitations in the Mott state. Hole-like excitation (top) corresponds to a missing atom. Particle-like excitation (bottom) corresponds to an extra atom.

invariant perturbation, so it can only create excitations with the net momentum equal to zero. So lattice modulation can excite an amplitude mode at  $k = 0$  or a pair of the Bogoliubov excitations with the opposite momenta ( see fig. 6.9). Secondly, it can be shown [5, 6] that lattice modulation does not couple to Bogoliubov excitations in the long wavelength limit. Roughly the argument is that Bogoliubov modes correspond to density fluctuations, whereas modulation of tunneling does not couple to the density. Thus even in the SF state the peak of the absorption spectrum is at finite frequencies: this is the combination of the amplitude mode and pairs of Bogoliubov excitations from near the zone boundary (phase space also favors exciting large  $q$  modes). Note that these experiments do not show mode softening at the transition. Close to the SF/Mott transition the energy of the amplitude mode becomes smaller but its coupling to lattice modulation in the long wavelength limit becomes suppressed. This is not surprising since at the point of the SF/Mott transition the amplitude mode is essentially the same as the phase mode (when there is no expectation value of the order parameter we can not separate longitudinal and transverse fluctuations).

Experimental observation of the amplitude mode would be really exciting. Especially if we could see the mode softening to demonstrate the basic feature expected at the quantum phase transition. A question of the damping of the amplitude mode is not resolved theoretically. It is expected that the mode remains underdamped in  $d=3$  but may be overdamped in lower dimensions.

Another possible probe of the amplitude mode would be to change parameters in the SF state and observe oscillations of the order parameter. This would appear as oscillations in the number fluctuations as measured by Bakr et al. [8]. The main difficulty of such experiments would be inhomogeneous confining potential. Different parts of the system would oscillate at different frequencies so the net oscillations could be strongly suppressed. Experimental resolution also requires finite strength of change in the parameters which quickly takes us outside of the harmonic theory.

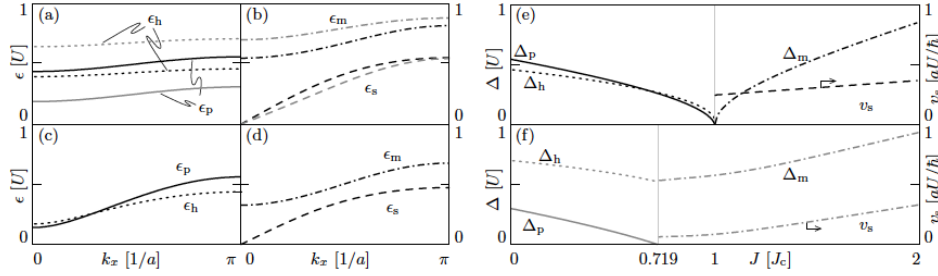


Figure 7.8: Collective modes in the Bose Hubbard model. Figure (a) and (c) show the dispersion of hole- and particle like excitations for different values of the interaction and the chemical potential. Figures (b) and (d) show dispersions of the amplitude and the phase modes. Figure (e) shows the change in the spectrum across the SF/Mott transition as the system is tuned through the tip of the Mott lobe (particle-hole symmetric case). Figure (f) shows a change in the spectrum across the SF/Mott transition when the Mott lobe boundary is crossed through its side (this is the p-h asymmetric case). Figure taken from [5].

## 7.5 Extended Hubbard models

One can also consider extensions of the Hubbard model to non-local interactions. For example, if we add nearest-neighbor interactions we have

$$\mathcal{H} = -t \sum_{\langle ij \rangle} b_i^\dagger b_j + \frac{U}{2} \sum_i n_i (n_i - 1) + V \sum_{\langle ij \rangle} n_i n_j - \mu \sum_i n_i \quad (7.36)$$

Hamiltonian (6.36) allows a new type of an insulating state: a checkerboard state shown in fig 6.11. This state breaks lattice translational symmetry. Transition from the superfluid to the checkerboard phase involves going from one spontaneously broken symmetry to another (number conservation in the SF to translational symmetry in the CB). Thus it is natural to expect the appearance of the intermediate phase where both are broken. This is called the supersolid phase. This phase has been predicted from the Gutzwiller analysis [14] (see fig. 6.12) and verified in the Monte-Carlo calculations [12]. Such phases are expected to be relevant for polar molecules in optical lattices [7].

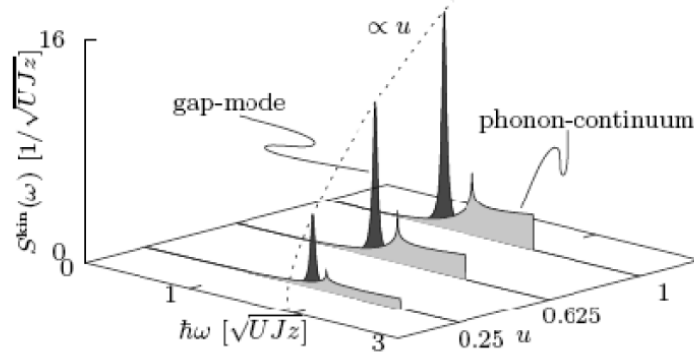


Figure 7.9: Theoretical analysis of the energy absorption spectrum in lattice modulation experiments in the bosonic Hubbard model. Lattice modulation can excite the amplitude mode at  $k = 0$  or a pair of Bogoliubov modes with the opposite momenta (so that the net momentum deposited into the system is zero). Bogoliubov modes with large momenta are predominantly excited. Hence absorption spectrum is dominated by the finite energy peaks even in the superfluid state. Deeply into the superfluid regime the intensity of the amplitude ("Higgs") mode peak is strongly reduced. Figure taken from [6].

## 7.6 Problems for Chapter 6

### Problem 1

In this problem you will analyze effects of interactions on the Bloch dynamics of Bose-Einstein condensates in one dimensional optical lattices. Hamiltonian of the system is given by

$$\mathcal{H} = -\frac{J}{2} \sum_{\langle lk \rangle} b_l^\dagger b_k + U \sum_l n_l(n_l - 1) - dF \sum_l l n_l \quad (7.37)$$

here  $J$  is the hopping,  $U$  is the interaction strength,  $d$  the lattice period,  $F$  magnitude of the static force.

a) Show that Hamiltonian (6.37) leads to a lattice version of the GP equation

$$i\dot{b}_l = -\frac{J}{2}(b_{l+1} + b_{l-1}) + U|b_l|^2 b_l - dF l b_l \quad (7.38)$$

b) Introduce new variables

$$b_k = \frac{1}{\sqrt{L}} \sum_{l=1}^{l=L} e^{ikl - i\omega_B l t} b_l \quad (7.39)$$

where  $\omega_B = dF$  is the Bloch frequency. Show that GP equations (6.38) can be

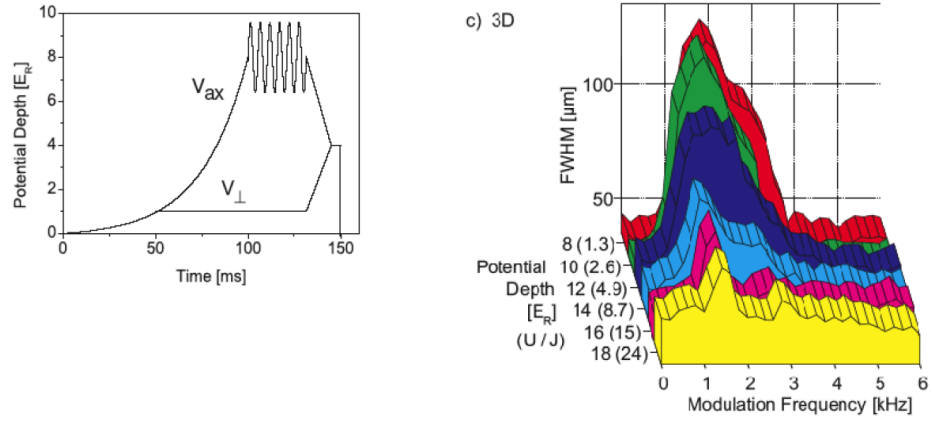


Figure 7.10: Lattice modulation experiments across the SF/Mott transition. Figure taken from [13].

written as

$$i\dot{b}_k = -J\cos(dk - \omega_B t)b_k + \frac{U}{L} \sum_{k_1, k_2, k_3} b_{k_1} b_{k_2}^\dagger b_{k_3} \delta(k - k_1 + k_2 - k_3) \quad (7.40)$$

Equation (6.40) allows a trivial solution

$$b_0(t) = \exp\left(i\frac{J}{dF} \sin(\omega_B t) - i\frac{UN_0}{dL}t\right) \quad (7.41)$$

What is the physical interpretation of this solution?

c) By linearizing equations (6.38) around the mean-field solution (6.41) we obtain

$$\begin{aligned} i\dot{b}_{+k} &= -J\cos(dk - \omega_B t)b_{+k} + 2\frac{U}{L}|b_0|^2 b_{+k} + \frac{U}{dL}b_0^2 b_{-k}^* \\ i\dot{b}_{-k} &= -J\cos(dk - \omega_B t)b_{-k} + 2\frac{U}{L}|b_0|^2 b_{-k} + \frac{U}{dL}b_0^2 b_{+k}^* \end{aligned} \quad (7.42)$$

Use these equations to calculate the decay rate of Bloch oscillations. Perform numerical analysis for  $U = 0.4$ . Calculate the decay rate as a function of  $kd$  and  $F$ .

*Hint* : Introduce the Floquet matrix

$$V = T_t \exp[-iU \int_0^{T_B} \begin{pmatrix} 1 & f(t) \\ -f^*(t) & -1 \end{pmatrix} dt] \quad (7.43)$$

where  $T_t$  denotes time ordering,  $T_B = 2\pi/\omega_B$ , and

$$f(t) = \exp(i\frac{2J}{dF}[1 - \cos(dk)]\sin(\omega_B t)) \quad (7.44)$$



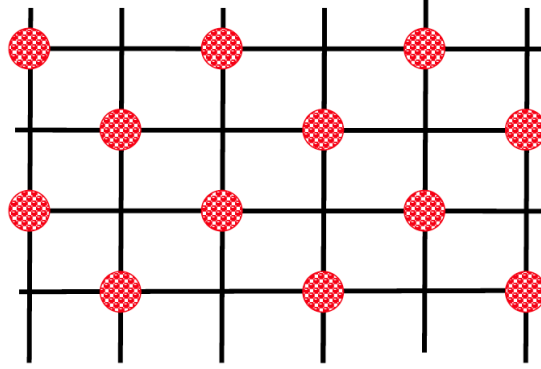


Figure 7.11: Checker-Board state. Insulating state that appears for nearest neighbor interactions. Unlike the Mott state it has a spontaneously broken symmetry: lattice translational symmetry.

Consider the maximal eigenvalue of the Floquet matrix  $V$  and relate it to the solution of the form  $b_{\pm k}(t) \sim \exp(\nu t)$ .

d) *More difficult problem.* One can use Feshbach resonance to change the contact interaction. When the s-wave scattering length is tuned to zero one is still left with magnetic dipolar interactions. In this problem you need to analyze the residual value of the decay rate of Bloch oscillations due to dipolar interactions. To solve this problem you also need to include transverse degrees of freedom. For simplicity assume layers to be infinite, so excitations can be characterized by the in-plane momentum  $\vec{q}$ .

Use the following form of effective dipolar interactions:

Intralayer interaction

$$V_0(q) = \frac{2U_d}{W\sqrt{2\pi}} - \frac{3U_d}{W\sqrt{2\pi}} F(|\vec{q}|) \quad (7.45)$$

Interlayer interaction for layers  $l$  lattice constant apart from each other

$$V_l(q) = -\frac{3U_d|\vec{q}|}{2} \exp\{-|\vec{q}|ld\} \quad (7.46)$$

Here  $W$  is the thickness of individual layers,  $U_d$  is the strength of dipolar interaction,  $\vec{q}$  is the in-plane momentum,  $F(x) = \sqrt{\frac{\pi}{2}} W |\vec{q}| [1 - \text{Erf}(\frac{Wq}{\sqrt{2}})] e^{q^2 W^2/2}$ , where  $\text{Erf}(x)$  is the error function. These expressions assume that dipolar moments are perpendicular to the planes and take into account finite width of individual layers. Formula (6.46) applies when  $W \ll d$ .

### Problem 2

Consider Hubbard model with nonlocal interactions

$$\mathcal{H} = -t \sum_{\langle ij \rangle} b_i^\dagger b_j - \mu \sum_i n_i + U \sum_i n_i(n_i - 1) + V_1 \sum_{\langle ij \rangle} n_i n_j + V_2 \sum_{\langle\langle ik \rangle\rangle} n_i n_k \quad (7.47)$$

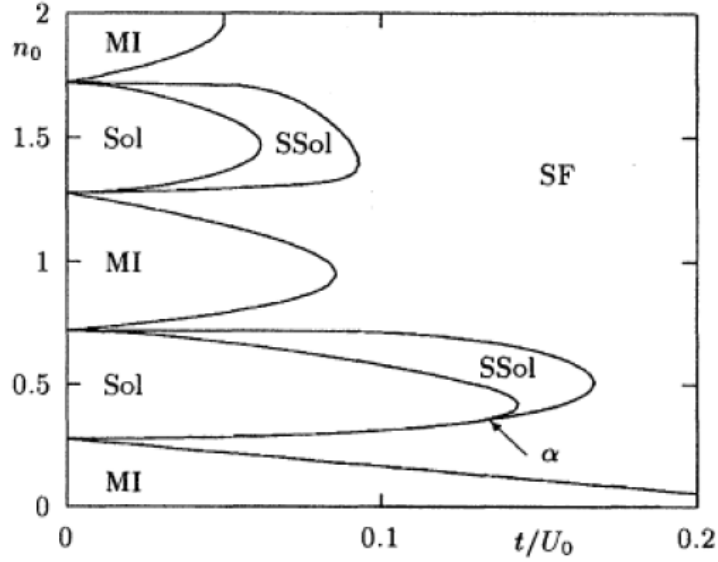


Figure 7.12: Phase diagram of the extended Hubbard model with on-site and nearest neighbor interactions. Sol denotes the checkerboard phase, SSol denotes the supersolid. Figure taken from [14].

In the limit when  $U$  is large we can keep states with occupations 0 and 1 only. This is known as the limit of hard-core bosons.

a) Show that in this limit Hamiltonian (6.47) can be mapped to the spin model

$$\mathcal{H} = -t \sum_{\langle ij \rangle} (S_i^x S_j^x + S_i^y S_j^y) - h \sum_i S_i^z + V_1 \sum_{\langle ij \rangle} S_i^z S_j^z + V_2 \sum_{\langle\langle ik \rangle\rangle} S_i^z S_k^z \quad (7.48)$$

Discuss the relation between various spin ordered states of (6.48) and insulating/superfluid/supersolid states of original bosons.

b) Use Curie-Weiss type mean field approach to study the phase diagram of (6.48). Assume  $V_2 = 0$ . Keeping  $V_1$  fixed plot the phase diagram as a function of  $\mu$  and  $t$ .

c) Extend analysis of part b) to finite  $V_2$ .

### Problem 3

In this problem you will consider collapse and revival experiments with (spinless) bosonic atoms in an optical lattice (M. Greiner et al. (2002)). The system is prepared in a superfluid state. You can take this initial state to be a product

of coherent states for individual wells

$$\begin{aligned} |\Psi(t=0)\rangle &= \prod_i |\alpha\rangle_i \\ |\alpha\rangle &= e^{-|\alpha|^2/2} \sum_n \frac{\alpha^n}{\sqrt{n!}} |n\rangle \end{aligned} \quad (7.49)$$

where  $|n\rangle$  is a Fock states with  $n$  atoms in a well. At  $t = 0$  the strength of the optical lattice potential is suddenly increased to a very large value, so that different wells become completely decoupled. You can take the Hamiltonian in this regime to be

$$\mathcal{H} = \frac{U}{2} \sum_i n_i(n_i - 1) \quad (7.50)$$

After the system evolves with the Hamiltonian (6.50) during time  $t$ , the TOF measurement is performed: both the periodic and parabolic confining potentials are removed, atoms expand freely, and image of the cloud is taken after long expansion.

a) Show the amplitude of interference peaks in the TOF images "collapses" after some time  $t$  then "revives", and then this cycle continues. Calculate both collapse and revival times.

b) Show that half-way between revivals the system goes through the so-called "cat state", in which  $\langle b \rangle = 0$  but  $\langle b^2 \rangle \neq 0$ .



# Bibliography

- [1] F. Greiner et. al. *Nature*, 415:39, 2002.
- [2] Gerbier et. al. *Phys. Rev. Lett.*, 101:155303, 2008.
- [3] J. Sherson et. al. *Nature*, 467:68, 2010.
- [4] N. Gemelke et. al. *Nature*, 460:995, 2009.
- [5] S. Huber et. al. *Phys. Rev. B*, 75:85106, 2007.
- [6] S. Huber et. al. *Phys. Rev. Lett.*, 100:50404, 2008.
- [7] T. Lahaye et al. *Rep. Prog. Phys.*, 72:126401, 2009.
- [8] W. Bakr et. al. *Science*, 2010.
- [9] Matthew P. A. Fisher, Peter B. Weichman, G. Grinstein, and Daniel S. Fisher. Boson localization and the superfluid-insulator transition. *Phys. Rev. B*, 40(1):546–570, Jul 1989.
- [10] R. Jackiw and A. Kerman. *Phys. Lett. A*, 71:158, 1979.
- [11] D. Jaksch, C. Bruder, J. I. Cirac, C. W. Gardiner, and P. Zoller. Cold bosonic atoms in optical lattices. *Phys. Rev. Lett.*, 81(15):3108–3111, Oct 1998.
- [12] Pinaki Sengupta, Leonid P. Pryadko, Fabien Alet, Matthias Troyer, and Guido Schmid. Supersolids versus phase separation in two-dimensional lattice bosons. *Phys. Rev. Lett.*, 94(20):207202, May 2005.
- [13] Thilo Stöferle, Henning Moritz, Christian Schori, Michael Köhl, and Tilman Esslinger. Transition from a strongly interacting 1d superfluid to a mott insulator. *Phys. Rev. Lett.*, 92(13):130403, Mar 2004.
- [14] Anne van Otterlo, Karl-Heinz Wagenblast, Reinhard Baltin, C. Bruder, Rosario Fazio, and Gerd Schön. Quantum phase transitions of interacting bosons and the supersolid phase. *Phys. Rev. B*, 52(22):16176–16186, Dec 1995.